

ASSESSMENT OF FRACTURING TUNNEL LININGS WITH SMEARED CRACK MODEL

Z.S. Wu¹, J. Yin¹, T. Asakura² and Y. Kojima³

¹Department of Urban & Civil Engineering, Ibaraki University, Japan

²Department of Earth Resources Engineering, Kyoto University, Japan

³Structural Technique Development Division, Railway Technical Institute, Japan

ABSTRACT

A finite element simulation is carried out to study the fracturing behavior of concrete tunnel linings with smeared crack model. To simulate the crack localization observed in experiment, a numerical strategy is introduced. Some weak elements as structural imperfections are inserted at critical positions of the tunnel linings to avoid the unrealistic crack distribution cracks due to the limitation of smeared crack model itself and the structural features of tunnel linings. It is found that the crack characteristics and structural performances of tunnel linings can be well simulated and predicted by smeared crack model with the numerical strategy on crack localization. In addition, the effect of a key material parameter, fracture energy, on the structural response of the tunnel linings is discussed.

KEYWORDS concrete tunnel linings, smeared crack model, fracture energy, crack localization, load-carrying capacity

INTRODUCTION

In Japan, there are currently thousands of railway and road tunnels in service. Many of them are being suffered from aging and external force, such as earthquake and traffic loading. Therefore, there exist serious problems on how to efficiently inspect and repair them to extend their service life. For this purpose, much work are being carried out experimentally [1,2], as well as numerical simulation [3], to study the mechanism of tunnel deformation and fracturing behavior. In this paper, the scale model experiments [1] is reviewed and referred. Smeared crack model is used to simulate the cracking behavior of the concrete tunnel linings. The objective is to obtain a general understanding of the effect of crack distributions on structural performance of plain concrete tunnel linings and the applicability of smeared crack model for the simulation on crack localization in such a structure.

EXPERIMENTAL REVIEW

A 1/3 scale model of plain concrete tunnel lining, as shown in Figure1, was tested. A tunnel lining specimen was supported by the I-shaped steel beams. No soil mass constrain outside the sidewalls was arranged. The external load was acted vertically down at the outside crown. This kind of load condition approximates the 2-dimension case.

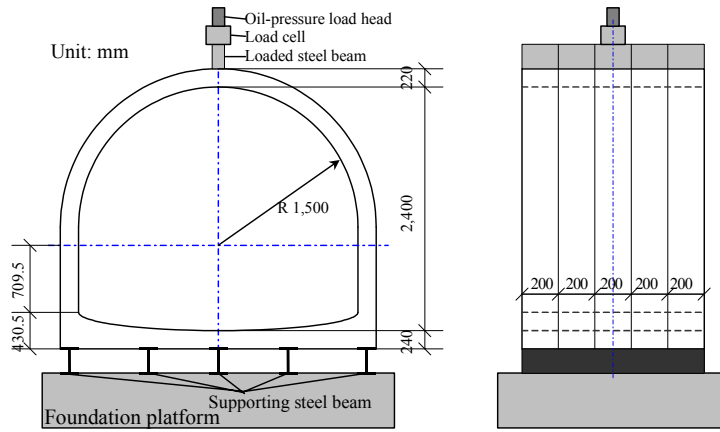


Figure 1: Cracks observed in experiments

According to the experimental observation [1], all the cracks that caused by the vertical load are flexural cracks. The first crack occurred in the crown (inside) followed by the ones occurring at the outside of sidewalls and the inside of bottom, as presented in Figure 2.

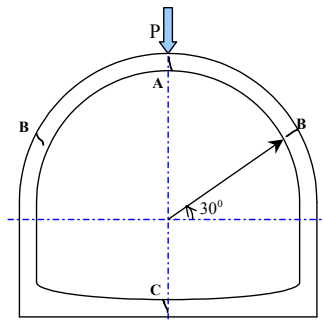


Figure 2: Cracking behavior observed in experiment

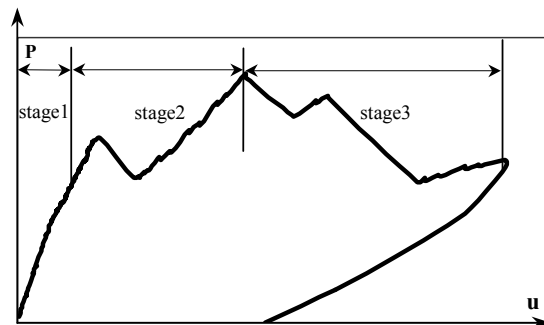


Figure 3: Four stages of tunnel lining response

From the load-displacement curve of experimental results, as shown in Figure 3, the structural stiffness decreased after the crack occurred at the inside of crown. But the tunnel lining could still resist the external load until the cracks happened at the outside of sidewalls. When the cracks at the sidewalls propagated to a certain extent, the tunnel lining began to lose its load resistance with the continuous deformation up to the ultimate collapse. A possible reason of the zigzag behavior in the experiment may result from unloading due to localized crack propagation. It can be seen that the structural response can be divided into 3 stages: 1) elastic stage with constant stiffness; 2) nonlinear stage after cracking occurrence with gradually decreased stiffness (but still positive); 3) strength degradation stage with negative stiffness until ultimate structural collapse.

The material properties obtained from identified uniaxial compression test are uniaxial compressive strength $f_c = 26.2\text{MPa}$, Young's modulus $E = 2.3 \times 10^4\text{MPa}$ and Poisson ratio $\nu = 0.17$ [1]. As a reference property, the tensile strength f_t can be calculated through transformation equation $f_t = 0.23f_c^{2/3} = 2.03\text{MPa}$, based on the concrete design standard of JSCE.

SMEARED CRACK MODEL

A finite element formulation of smeared crack model [4] is used in the simulation. But, the treatment on the variation of shear modulus along the crack plane is modified by applying a softening curve rather than using conventional constant shear retention factor. The relation between the crack strain increment Δe^{ck} and the stress increment Δs can be defined as

$$\Delta s = D^{ck} \Delta e^{ck} \quad (1)$$

where D^{ck} contains the local stress-strain relations normal to and along the crack plane. It could be written as

$$D^{ck} = \begin{bmatrix} D^I & 0 \\ 0 & D^{II} \text{ (or } D_0^{II}) \end{bmatrix} \quad (2)$$

in which D^I is mode I tensile softening modulus, D^{II} is mode II shear softening modulus and D_0^{II} is the initial shear modulus before the mode II softening is entered, as shown in Figure 4. According to crack band theory [5], the actual discontinuous displacements on the crack plane, δ_n for opening and δ_t for sliding, are smeared over the a band of width h . Therefore, the crack strains $e^{ck} = \delta_n/h$ and $\gamma^{ck} = \delta_t/h$ are obtained. In the simple form, the crack band width h can be taken as an equivalent element size. For 2-dimension elements, h is approximated as $h = \sqrt{A}$, where A is the element area. Fracture energy is assumed to be a material property, defined as the energy required to bring a unit area to complete fracture. The areas below the local stress-strain curves at crack plane are the unit fracture energy over crack band h , G_f^I/h for mode I and G_f^{II}/h for mode II.

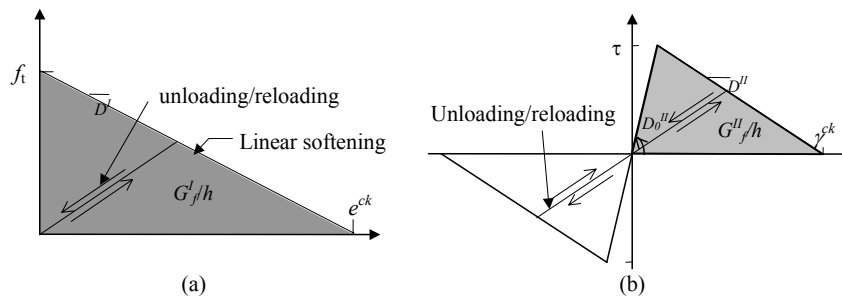


Figure 4: Softening models (a) Mode I tensile softening (b) Mode II shear softening

A linear tension softening curve is adopted for mode I fracturing. It is assumed that mode I fracture is initiated first when principle stress reaches the concrete tensile strength. Therefore, the shear stress across the crack is zero at the onset of cracking. That is why the shear stress-strain diagram in Figure 4(b) starts from the origin. Upon subsequent change of the principle stress axes the shear stress across the initial crack plane may increase until its maximum value τ , thereafter the shear softening branch is started. Different from the present treatment of mode II softening, in the traditional smeared crack model, a constant shear retention factor β is multiplied to the elastic shear modulus and kept unchanged in subsequent calculation. It may likely result in shear stress locking so as to lead to incorrect numerical results. Furthermore, the unloading and reloading are modeled by a secant path, which implies that the stress follows a linear path back to the origin.

NUMERICAL SIMULATION

A finite element code, in which smeared crack model is implemented, is used to carry out the numerical simulation. The structural model of tunnel lining, as shown in Figure 1, is discretized by 4-node plane stress elements. Strain and stress are integrated at 4 Gaussian quadratic points.

Treatments of Shear Modulus on Crack Plane

First, the difference between the proposed shear softening model and the traditional constant shear retention factor is compared. The constant shear retention factor with $\beta=0.5$, 0.1 and 0.01 is used respectively for the traditional post-tension crack treatment of shear modulus. Other common material properties are concrete tensile strength $f_t=1.8\text{MPa}$, mode I fracture energy $G_f^I=0.15\text{N/mm}$. For the shear softening model, initial shear retention factor is $\beta=0.5$, shear strength is $\tau=0.2\text{MPa}$ and mode II fracture energy is $G_f^{II}=0.01\text{N/mm}$. The results are shown in Figure 5.

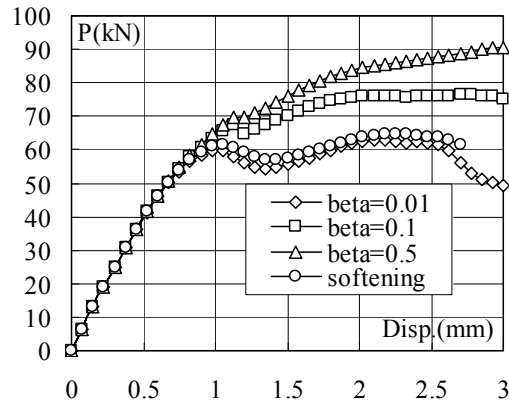


Figure 5: Different treatment of shear modulus

It is demonstrated that value of constant shear retention factor significantly influences the numerical results even though the mode II fracture is not dominant in the tunnel lining structure under such a load condition. Only the curve of case $\beta=0.01$ is close to the one of the shear softening model. In the viewpoint of concrete material behavior, the shear softening model is more physically reasonable because concrete is quasi-brittle material and the shear modulus dose not likely drop dramatically at the onset of the opening crack. In the following simulations, the mode II softening model is adopted.

Effect of Initial Imperfection

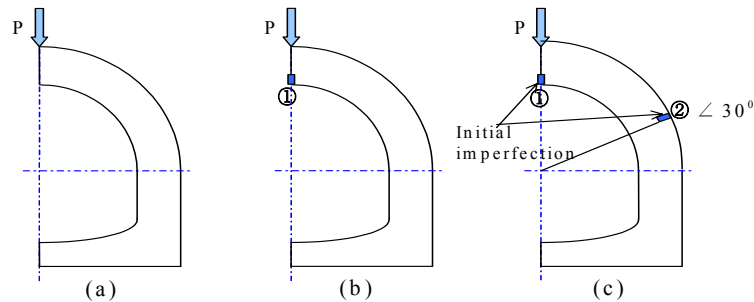


Figure 6: Initial imperfection at different positions

From the experimental observations, the localized cracks are mainly located at the following positions: 1)inside of crown, 2)outside of sidewalls, and 3)bottom of tunnel. Three cases are used to study the effect of the initial imperfection in the numerical simulation by smeared crack model, as shown in Figure 6: (a) without any initial imperfection, (b) with initial imperfection only at inside crown ① and (c) with initial imperfection positions ①+②. Since the crack that happens at the bottom does not further propagate, its effect on the structural behavior is not discussed in this paper. The initial imperfection is inserted by weakening one tip element with 1/2 concrete tensile strength and 1/4 fracture energy G_f^I of the normal ones. Concrete properties are tensile strength $f_t=1.8\text{MPa}$, mode I fracture energy $G_f^I=0.15\text{N/mm}$.

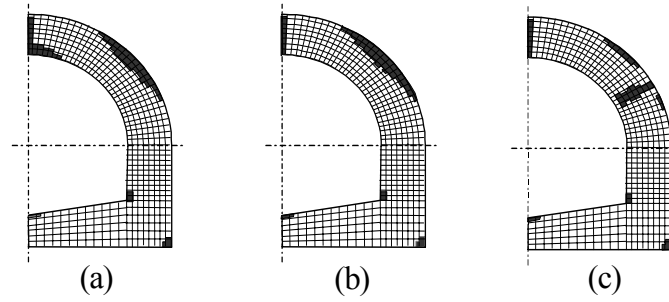


Figure 7: Crack patterns with and without initial imperfections

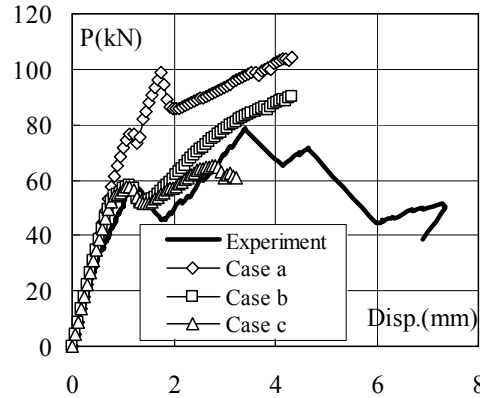


Figure 8: Load-displacement curve with and without initial imperfection

The simulation results of crack patterns and load-displacement curves are shown in Figure 7 and 8. Figure 7(a) (b) and (c) correspond to the case (a) (b) and (c) in Figure 6, respectively. Without any initial imperfection, cracks are widely distributed at the outside of sidewalls. Since the localized crack does not form, the local unloading behavior could not be found in load-displacement curve. This may result from two reasons. One comes from the deficiency of the smeared crack model, which smears a realistic crack over the whole finite element. This easily leads to the distributed crack. The second reason may be due to the gentle stress distribution in the tunnel lining under such a vertical load. The arch-shaped structure makes the stress gradient along the sidewalls relatively small. This also causes the difficulty during FE simulation of crack propagation. By using the numerical strategy with weak elements at critical positions, it is found that crack localization can be simulated by smeared crack model.

Concrete Fracture Energy

Fracture energy, G_f^I , is generally considered as a material property, which is defined as the amount of energy required to create a unit area of mode I crack. Because there is not much experimental data of the fracture energy, 5 cases with fracture energy $G_f^I=0.10, 0.15, 0.20, 0.40$ and 1.00N/mm are simulated. The results are compared to the experimental one. Concrete tensile strength is $f_t=1.8\text{MPa}$.

The load-displacement curves are presented in Figure 9. It can be seen that when fracture energy is relatively small with $G_f^I=0.10, 0.15, 0.20\text{N/mm}$, cracks propagate rapidly after initiated. Because the stress on the crack plane releases rapidly, the local unloading behavior is apparently seen when cracks develop at crown and at sidewalls respectively. However, in the case of higher fracture energy $G_f^I=0.40, 1.00\text{N/mm}$, such an unloading behavior is not clearly shown out. With increase of fracture energy, not only the load-carrying capacity is enhanced, but the crack patterns also change even though the weak elements are inserted in the same critical positions as discussed previously. The area of cracked elements elsewhere also increases, as shown in Figure 10. Therefore, increasing the fracture energy of concrete by some means could effectively enhance the load-carrying capacity and prevent excessive crack localization in tunnel linings.

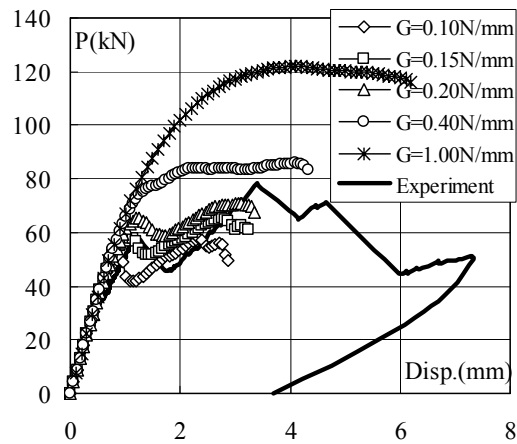


Figure 9: Load-displacement curve with different fracture energy

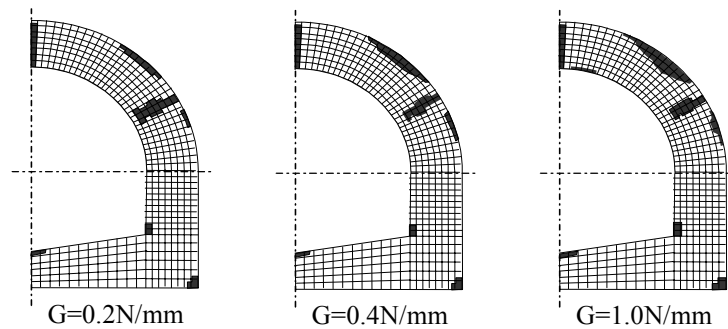


Figure 10: Change of crack patterns with increase of fracture energy

CONCLUSION

Through the numerical simulation with smeared crack model, the cracking behavior of concrete tunnel linings is studied. Shear softening model is used, in place of constant shear retention factor, as a rational approach to treat shearing behavior on the crack plane. As to smeared crack model, it is generally considered not so applicable to simulate localized cracking in complicated structures such as tunnel lining. But, by inserting weak elements at critical positions, such a disadvantage is overcome, and characteristics of cracking behavior and structural response are well simulated. In addition, the significance of fracture energy is discussed. Increasing the fracture energy of concrete tunnel lining intends to result in distributed crack so that it can effectively enhance the load-carrying capacity and deformation. This finding might be helpful to tunnel lining design in the future.

REFERENCE

1. Asakura, T., Ando, T. and Kojima, Y. (1998): Experiments of inner reinforced tunnel linings, *QR of RTRI*, Railway Technical Institute, Japan
2. Asakura, T., Kojima, Y., Ando, T., Sato, Y. and Matsuura, A. (1994) *J. of Geotech. Eng. JSCE* No.493/III-27, pp.79-88.
3. Yin, J., Wu, Z.S., Asakura, T. and Ota, H. (2001) *Structural Eng./Earthquake Eng. JSCE* Vol.18, pp.17-27.
4. de Borst, R. and Nauta, P. (1985): Smeared crack analysis of reinforced concrete beams and slabs failing in shear, *Proc. Int. Conf. on Computer Aided Analysis and Design of Concrete Struc.*, pp.261-273, Damjanic, F. et.al (Eds). Part 1, Prineridge Press, Swansea.
5. Bazant, Z. (1984) *J. of Eng. Mech. ASCE*, Vol.110, No.4, pp.518-535.